

Underwater wireless sensor nodes for ecosystem monitoring applications using two-layer binary traversal based optimal image compression technique

Danesh K^{a*} & Dharani R^b

^aDepartment of Electronics and Communication Engineering, SRMIST (Ramapuram Campus), Chennai 600 089, India

^bDepartment of Information Technology, Panimalar Engineering College, Chennai, 600 123, Tamilnadu, India

Received: 26 August 2023; Accepted: 5 April 2024

In current years, underwater wireless sensor networks (UWSNs) have attracted huge attention from researchers. Generally, UWSN encompasses a huge quantity of sensors, and underwater vehicles are collaboratively arranged for performing the collection of data, interpretation, and, processing. However, its difficult nature makes position updates or including new devices more challenging. Moreover, owing to the limitations of UWSN energy storage of end devices, restricted bandwidth, and its difficulty in recharging or repairing the underwater device, this is extremely important to improve the energy performance of UWSN. The power consumption imbalance can cause restricted network lifetime and less performance. In order to overcome these issues, an optimal threshold-driven image compression approach is proposed in UWSN. The run length encoding model is applied for improving the compression performance in UWSN. The performance of the designed optimal image compression approach is assessed by means of various performance measures, such as compression time (s), decompression time (s), space-saving (%), and compression ratio, Peak Signal to Noise Ratio (PSNR), Signal to Noise Ratio (SNR), Mean Square Error (MSE), Structural Similarity (SSIM), and Mean Absolute Error (MAE). Thus, the devised image compression model attained less, compression time, compression ratio, decompression time, MSE, and MAE of 5.426, 2.0294, 5.064, 0.0550, and 0.141, respectively.

Keywords: Image compression, Underwater wireless sensor node, Image reconstruction, SSIM, MSE

1 Introduction

Wireless Sensor Networks (WSNs) have grown in popularity as a research topic due to their applications in a variety of fields, including disaster management, smart cities, wearable, autopilot, smart buildings, agricultural drones, and border surveillance¹⁻²³. Usually, WSNs encompass huge amount of devoted, free, and dense sensors randomly organized in the sensing field for monitoring physical phenomena in an environment^{22,24,27}. Every sensor node comprises four major elements: processing element, sensing component, power supply, and communication element^{2,30}. WSN has been effectively employed in various areas, like medical investigation, surveillance, disaster management, home automation, and military battlefield^{3,4,5}. Although WSN has the issue in managing large quantities of image data owing to energy limitation and bandwidth. For the more complicated the process, more energy is required^{6,26,28}. The Earth's ecology is primarily made up of water, and it includes more than 75% of its surface. Water covers Earth in numerous varieties, including lakes, rivers, and oceans, and it is

essential to human life and other animals. Usually, water occupies above 75% of earth's surface and most underwater regions are yet to be discovered^{7,20}. To achieve this process, UWSN has been extensively employed. These underwater sensor nodes are organized in seas or rivers for identifying features existing in water environment, like current flow, water quality, pressure, and temperature. Moreover, it has more applications, like exploration, monitoring, and underwater communication. Although UWSN has processing abilities and restricted resources⁸. The underwater sensor node can be utilized for measuring underwater features, like acidity, conductivity, hydrogen, turbidity, density, temperature, chemicals, pH, and melted methane gas^{9,21}.

Besides several underwater applications have been researched in recent years, for example, disaster prevention, undersea explorations, mine investigation, environmental monitoring, and so on. However, devised traditional monitoring approaches are more complex and expensive. These tools exploit individual and detached apparatus for collecting data from their nearby environments. The development of UWSN affords novel opportunities for exploring the ocean. The costly, predictable huge, individual ocean

*Corresponding author (E-mail: danesh.knl@gmail.com)

monitoring tools are changed by moderately small and also less luxurious underwater sensor nodes in UWSN, which can communicate with others through acoustic signals¹⁰. Furthermore, it has been newly utilized to collect underwater visual data, like videos and images with the development of tele-monitoring and communication technologies of UWSN. In order to assist this procedure, various sensor nodes and also vehicles with cameras are organized in the distribution method. However, the surveillance action necessitates enduring distribution of sensor nodes. Nevertheless, providing power to battery-operated nodes becomes serious problem because nodes cannot be exchanged frequently. The major resolution is to compress the data; it must be carried out in a sensor processor^{1,17}.

Commonly, there are three types of sensor nodes in UWSN, such as unknown, anchor, and reference nodes. The anchor nodes are answerable for localizing unfamiliar nodes, whereas unknown nodes are in charge to localize unknown nodes. Besides, they can obtain the location in advance based on artificial arrangements and GPS systems. In addition, reference nodes comprise initial anchor and localized unidentified nodes. More approaches have been researched for UWSN for example; secure routing methods, time synchronization schemes, Medium Access Control (MAC), and localization schemes^{10,25}. Moreover, routing approaches for UWSN have two kinds, namely localization-free and localization-based systems^{18,19}. The localization-free model utilizes depth quantity of sensor node for creating routes to sink. Meanwhile, localization-driven schemes need node position for finding routing path from node to sink. Besides, sensor node depth is evaluated based on pressure sensors furnished on nodes. Usually, localization-free method has more benefits than other systems with regard to scalability. Owing to node mobility, routes can be formulated based on depth, if network topology varies^{9,29}.

The motivation behind developing a two-layer binary traversal-based optimal image compression technique stems from the necessity to efficiently utilize the limited resources available in these nodes. Underwater environments present unique challenges such as limited bandwidth, and energy constraints. By employing a two-layer binary traversal approach, the technique aims to reduce the size of image data while preserving important visual information. This compression technique can significantly improve the efficiency of data transmission, reduce energy

consumption, and enable longer operation times for underwater sensor nodes, thereby facilitating effective and sustainable ecosystem monitoring in underwater environments.

The major contribution of this research is to design and develop an optimal image compression approach in UWSN. Here, the optimum threshold-driven image compression approach affords better band width utilization and enhances the performance of compression during energy consumption is reduced in sensor nodes. In the compression process for underwater wireless sensor nodes, the sensor tracks underwater images and converts them into pixel rates. These rates are encoded in 8 bits using binary representation, reducing the encoding bits. Position-driven binary traversal generates two code words for each pixel rate based on 0s and 1s traversals, selecting the code word with minimal bits as the optimal code word for the next level. Compression performance is enhanced by employing run-length encoding. In decompression, the RLE decoding approach is used to decode the compressed file, and the bit-reduced and code word data obtained from the position traversal model during encoding are used in the decoding process. The reverse position-driven traversal approach is applied to rebuild the original image.

The most significant intention of this research work is elucidated as follows,

Developed optimum image compression model in UWSN: An optimum threshold-enabled image compression model is designed in UWSN for ecosystem monitoring applications. Moreover, the run length encoding approach is employed to enhance the performance of compression in UWSN.

The rest of research paper is organized as follows. Section 1 explains the literature review of UWSN. In section 2, proposed Two-Layer Binary Traversal based Optimal Image Compression Techniques examined in detail. Section 3 presents experimental outcomes of the newly developed compression technique are addressed along with a comparison. Finally, Section 4 provides the conclusion and future enhancement of this paper.

1 Related Works

The literature review related to image compression in UWSN is explicated in this section.

Neighbourhood Correlation Sequence (NCS) technique was devised in², for low complexity and highly reliable image compression process. In addition, this approach executes a bit reduction function and also

encoded was done by codec, like Deflate, and Lempel Ziv Markov chain model for compressing the image. This model improves the performance of compression as well as decreases energy utilization of sensor nodes along with better fidelity. This technique effectively improves average bit rate, PSNR and end-to-end delay. Furthermore, it maintains an improved trade-off between reconstructed image quality and compression effectiveness. Even though, encoding algorithm was not used for encoding the generated codewords.

The Coefficient Permuted Adaptive Block Compressed Sensing (CP-ABCS) was presented in⁷ to improve image reconstruction thoughtless samples. This model works in a sensor processor for compressing data in nodes after that, reduced data was transmitted. Block Compressed Sensing (BCS) driven image compression was utilized for improving sensor lifetime and saving energy. The transform coefficients were regularly distributed to each block for solving less sampling efficiency. Moreover, Adaptive BCS was employed in order to fix the samples selected from image blocks. This model attained better PSNR, space saving, and SSIM, but still it was not effective for real time scenarios.

An Energy-based Adaptive Block Compressive Sensing (EABCS)¹¹ was designed through an orthogonal matching pursuit reconstruction model for enhancing visual superiority of reconstructed image and sampling performance. Here, the sparse binary random matrix was employed as a dimension matrix, because it is highly sparse. Besides, high measurements were allocated to blocks along with high energy using energy driven adaptive scheme. This approach achieved better SSIM, PSNR, and space-saving percentages were also improved, still processing time was high in this method.

The Discrete Wavelet Transform (DWT) enabled deep learning approach was developed in¹² for image compression. The Convolution Neural Network (CNN) was employed for the encoding and decoding part for attaining better compression with improved reconstruction image quality. CNN model executes a learning procedure for affording optimal compact illustration of the original image, which holds structural data. The PSNR and space saving rate was high in this approach, although it was not implemented in practical setups. An adaptive node clustering routing model¹³ was proposed for smart ocean UWSN using an optimization approach. This network was separated into clusters, where the cluster head is elected based on existing energy in sensor

node. The re-transmission cause replicated packets or high latency at receiver when choosing cluster members. The routing cost was reduced in this approach, but the processing speed should be decreased.

Topology Control Energy Balance (TCEB) model was introduced for UWSN in¹⁴. This model considers the factors, like path loss and node energy for choosing cluster head. Moreover, topology control system is deliberated as non-cooperative game. Every node can become a cluster head based on various approaches and payoffs set for game. Besides, the payoff function is represented as residual energy function and path loss of one-hop distance as well as intent to balance energy consumption of every node. The network lifetime was highly increased and attained better performance in network load balancing. However, this approach failed to reduce end-to-end delay, while network scale was huge. In addition, a clustering protocol model was employed in¹⁵ for multi-hop routing in UWSN. This model permits the node for altering energy consumption when handling exceptional network performance. In addition, Energy Optimization Clustering Algorithm (EOCA) needs nodes for communicating with neighbors' ineffectual communication range. Here, every node computes the whole transmission delay among the sink, and the node after that chooses the cluster head based on the total transmission delay rate. This approach attained better packet delivery ratio with high lifetime, but still, energy consumption was high. An Energy-balanced Unequal Layering Clustering (EULC) technique was proposed in¹⁶ for UWSN in order to diminish consumption of energy in inter-cluster communications. Moreover, it implements UASN with unequal layering using node depth and also it solves hot spot problems by cluster generation with different size and same layer. This approach efficiently balances energy; thus, the lifetime of network was increased. However, this approach did not guarantee the data transmission security.

Even though there are several works already in existence, they have certain issues with real-time applications that need an enormous amount of bandwidth. The proposed approach regulates the trade-off between bandwidth utilization and visual quality adequately.

1.2 Challenges

- The Coefficient Permuted Adaptive Block Compressed Sensing (CP-ABCS) was proposed in for improving image reconstruction process

with fewer samples. However, this model was not implemented for real time underwater videos⁷.

- In NCS approach was introduced for low complexity with highly reliable image compression procedure. Although, this technique was not executed on Internet of Things (IoT) for managing constrained resources on computer vision applications².
- EABCS model was proposed in which improves the visual superiority of sampling performance and reconstructed image, even though it was not performed for underwater surveillance videos¹¹.
- DWT-based deep learning system was designed in, which performs effective image compression, but still it failed to utilize denoising process for enhancing the outcomes².
- In EULC model was devised for UWSN, it effectively reduces energy consumption in inter-cluster communications. However, this approach did not optimize network topology for improving energy efficiency¹⁶.

2 Material and Methodology

2.1 System Model

The general network set-up of UWSN has two kinds of nodes, first one is nodes, which know their position based on positioning format, named Beacon nodes and nodes that do not know their position is specified as unknown nodes. The amount of beacon nodes along with position information is minimal in nature, because UWSN is battery-controlled atmosphere and frequent replacement of sensor nodes battery is incredible. Therefore, there is a need for network model, which affords optimal performance in underwater circumstances³¹. In UWSN, limited bandwidth is one of the major problems due to the attenuation of signals in water. The available bandwidth in water is limited, which restricts the amount of data that can be transmitted. One of the solutions for limited bandwidth is to use data compression techniques to reduce the size of the data that is transmitted. Compression algorithms can reduce the size of the data without losing significant information. Data compression can be done using a novel optimal threshold-based compression technique for ecosystem monitoring applications. The system model of the proposed algorithm is depicted in Fig. 1. In compression process, sensor present in UWSN structure tracks the underwater images and the images are converted to pixels rates. After that, the pixel rates are

encoded in 8-bits in binary representation and the position driven binary traversal is applied, thus the encoding bits gets decreased. Moreover, two code words are generated for every pixel rate based on 0s and 1s traversals. The code word with minimal bits is chosen as optimum code word for next level and also traversal count is updated. In another level, the created code word is decreased by means of threshold of code word length. The compression performance in UWSN is improved by employing run length encoding. Additionally, symmetrical technique is applied along with decompression and compression function in this presence of inverse operation. In decompression process, RLE decoding approach is exploited for decoding compressed file. The bit-reduced as well as code word data attained from position traversal model on encoding section is outcome of decoding section. The reverse position driven traversal approach is utilized for rebuilding original image.

2.2. Proposed Optimal Image Compression Technique

The proposed Optimal Threshold-based Image Compression technique provides optimal bandwidth utilization. Also, improves compression performance while decreasing energy consumption in sensor nodes.

Consider, a two-dimensional input image A with $a_{r,c}$ pixels is given as,

$$A = \begin{bmatrix} a_{0,0} & a_{1,0} & a_{0,1} & a_{1,1} & \dots & \dots & a_{0,c-1} & a_{1,c-1} & \vdots \\ a_{r-1,0} & \vdots & a_{r-1,1} & \ddots & \dots & \vdots & a_{r-1,c-1} & \vdots & \vdots \end{bmatrix} \dots(1)$$

Where, r and c specifies row and column representation of input image A . Here, $r \times c$ offers whole resolution of image A (for example, 256×256 resolution), and $a_{r,c}$ represents pixel positioned in the r^{th} row and c^{th} column of two-dimensional input image A .

Most significantly, 8 bits are needed to denote every pixel rate in input image A a, that the pixel value ranges from. Therefore, in the first layer position-enabled binary traversal scheme provides a code-word, for the second layer we apply the threshold value to reduce the bit again to provide an optimal code-word. Further, to enhance the compression process, two-layered optimal code-words are encoded by run length encoding and generate the compressed data for transmission.

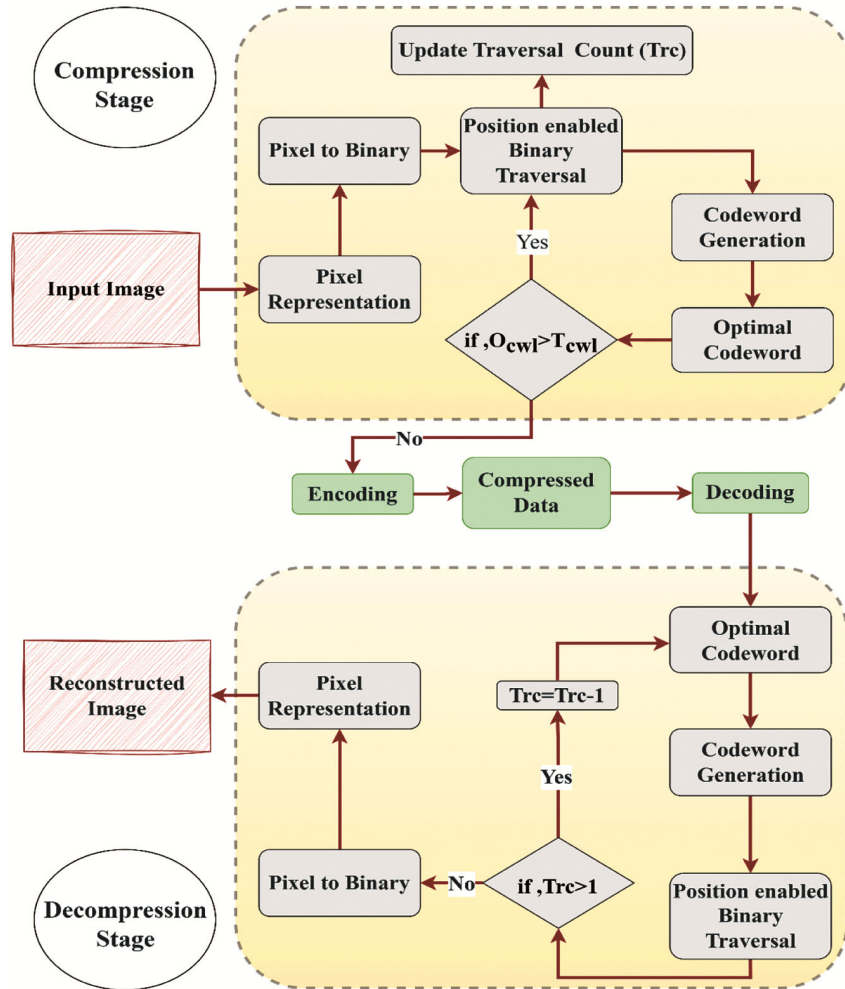


Fig. 1 — System model of compression in UWSN.

2.3 Compression process

The proposed method is a reliable, simple image compression methodology established specifically for UWSN sensor nodes with limited energy resources. At first, sensors in the UWSN environment track underwater images. Following that, these images are transformed into numerical (or pixel) values. Then, these pixel values are encoded in 8 bits in binary representation based on the following pseudo-code.

1. *set, n = 8*
2. *bit = 1*
3. *while (n > 0)*
4. *bin(bit) = mod(n, 2)*
5. *n = (n - rem(n, 2))/2*
6. *bit = bit + 1*
7. *end while*

Then, employing position-enabled binary traversal, the bits for encoding are reduced. The control bit is assigned as a 2-bit encoding format, depending on the

first bit in position-enabled binary traversal is represented in equations (2) and (3).

$$C_{bit_0} = \{00, 0 \text{ bit traversal} 01, 1 \text{ bit traversal} \dots\} \quad (2)$$

$$C_{bit_1} = \{10, 0 \text{ bit traversal} 11, 1 \text{ bit traversal} \dots\} \quad (3)$$

The control bit is stored as ‘00’ for 0-bit traversal and ‘01’ for 1-bit traversal when the first bit is zero. Similarly, the control bit is stored as ‘10’ for 0-bit traversal and ‘11’ for 1-bit traversal, when the first bit is one. The traversal method initiates at second bit as well as examines existence of 0s in binary series using first bit as a reference bit. When rate of 0s is discovered, associated locations are considered as part of first-level code-word. The positions are modified accordingly until all of the 0s in the sequence have been identified.

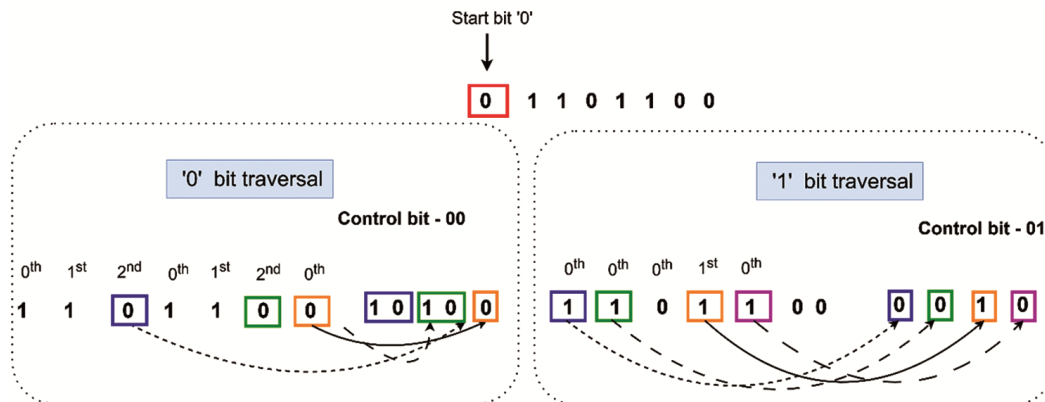


Fig. 2 — First level code-word generation.

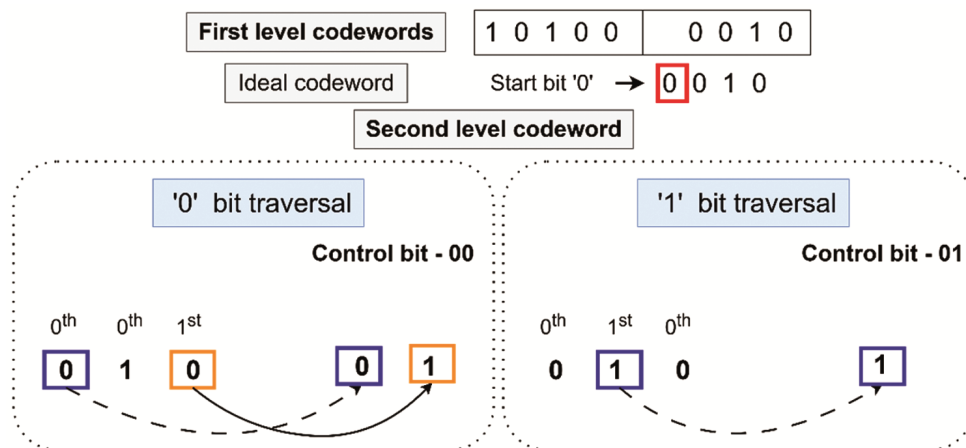


Fig. 3 — Second level code-word generation.

Likewise, 1s-based code-word was also generated. An illustration of the first-level position-enabled code-word is shown in Fig. 2. Two code-words are created for each pixel value using the 0sand1s traversals, respectively, which represent the presence of 0s and 1s in binary representation. Then, the code-word with the least bits is selected as an ideal code-word for the next level and the traversal count is updated.

In the second level, an above-generated code-word is reduced based on the code-word length threshold. The code-word above or equal to the threshold values, the particular code-word is considered for second-level bit reduction. Here the reduction is carried out by position-enabled binary traversal and the traversal

count along with measurement of the code-word is updated. The second level reduction is depicted in Fig. 3. The resulting code-words of total pixel rates are concatenated with control bits to create compressed file. Example of optimal code-word generation based on pixel values are tabulated in Table.1

In order to enhance the performance of compression in UWSN run-length encoding is employed. Run length encoding is an effective approach for compressing data where the same sequence appears repeatedly, such as an image with minimal variability. Also, useful for image compression since images have lengthy sequences of pixels with the same color. This technique looks for collections of identical bits, bytes, or pixels and encodes both their length and value. For example, the encoding of the string 0011 would be (0:2) (1:2). Then use Huffman coding to compress each (bit: length) as a single unit. This method performs best when the bit is repeated continuously. Finally, the compressed file is ready for transmission in UWSN. The overall compression procedure is depicted in Fig. 4.

2.4 Decompression process

The compressed file reaches the receiver and is ready for decompression. The proposed technique employs a symmetrical approach, with compression and decompression being inverse operations In order

Table 1 — Example of optimal code-word generation

Pixel Value	Binary Representation	Position Enabled Binary Traversal				Code-word	Optimized Code-word
		0-bit traversal		1- bit traversal			
		Control bit	Code-word	Control bit	Code-word		
137	10001001	10	00010	11	1110	1110	00
245	11110101	10	111	11	00011	111	111
112	01110000	00	11000	01	000	000	000
208	11010000	10	11000	11	01	01	01
95	01001110	00	1	10	010000	1	1
78	01011111	00	1011	010	01000	1011	0
51	00110011	00	0100	01	10100	0100	0
167	01101100	00	010	01	11000	010	010
108	10100111	10	10100	11	0010	0010	1

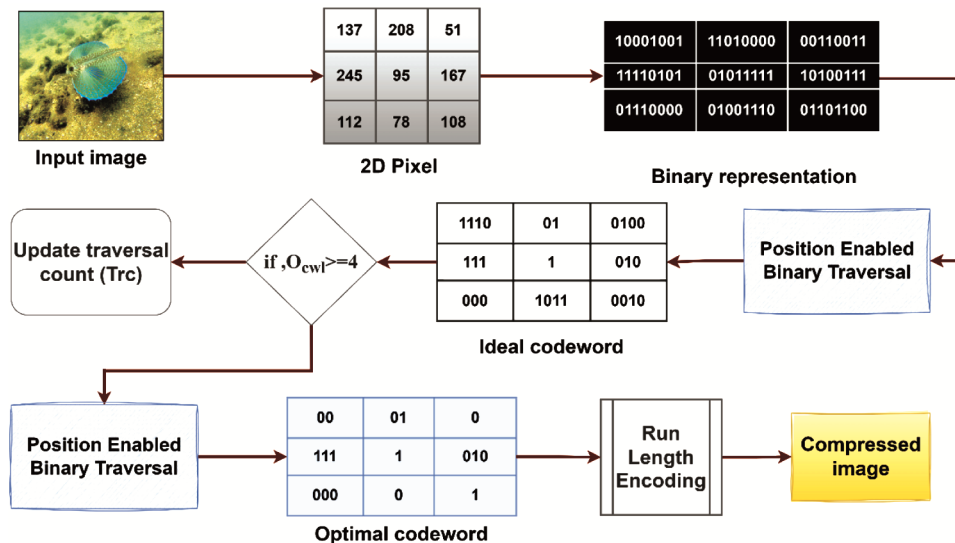


Fig. 4 — Overall compression process.

to decode the compressed file, the decompression process begins first and uses the RLE decoding method. The actual optimum code-word or bit-reduced data acquired from position traversal method on encoding part is output from decoding block. To rebuild the original image, the reverse position-enabled traversal method should be used. The optimal code-words encompass encoded pixel rates, are read using reverse position-enabled traversal technique. As previously stated, 2-bit encoding of control bit makes it easier to determine initial bit of binary series and whether code-word starts with 0s or 1s. For instance, control bit of 00 suggests, that first bit in 8-bit binary series is 0 and has been encoded using a 0-bit traversal. Once it is determined that the code-word is based on 0s, 0s values will be appended to the appropriate positions in binary arrangement, starting with first bit. Meanwhile, first bit can be determined

from control bits themselves, each position denoted by the code-words will be filled with values of 0, and residual locations will be occupied with values of 1.

Similarly, with 1-bit traversal, 1s are filled in every position indicated by the code-word, and 0s are filled in the rest of the positions. The code-word for a binary value is then correctly reconstructed and changed back to a pixel. After that, pixel values provide the reconstructed images. In precisely similar mode, all of code-words are decoded to effectively recreate original image. The above process is represented in the below Fig. 5.

2.5 Demonstration

For understanding, consider the example for a sample pixel value ‘78’ in Table 1. The proposed strategy will work in the following way: Initially, pixel rate ‘78’ is transformed into 8-bit binary format,

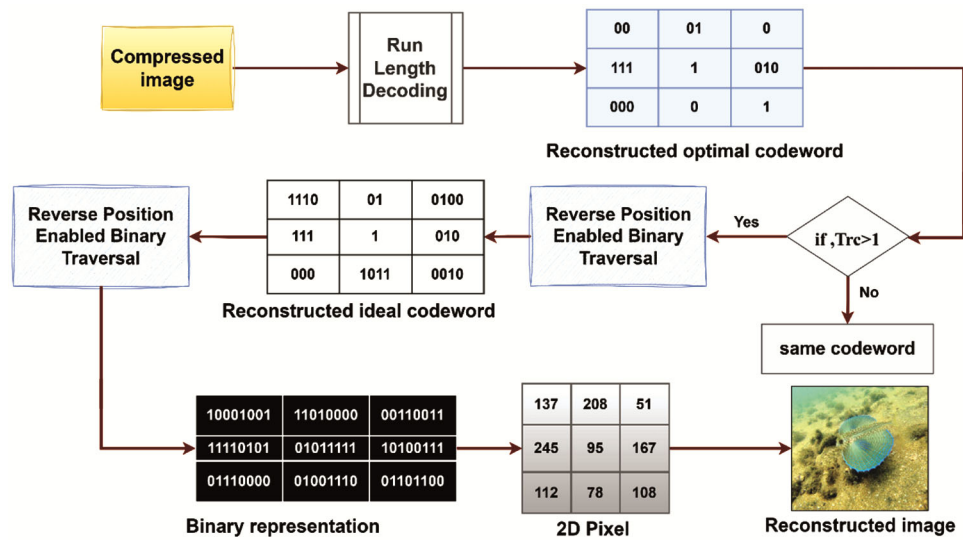


Fig. 5 — Overall decompression process.

which is “01001110”.The encoding procedure begins with initial bit of binary order and determines it as 0. Following that, a 0-bit traversal is started along with the control bit 00. With reference to the start bit, the 0-bit traversal locates all instances of 0 values, and the appropriate positions are kept as the code-word. Then, the following adjacent bit is intended to be in position 0, and the following bits are taken to be in positions 1, 2, and so on. Again, bit traversal begins from subsequent bit and recognizes 0 at the 1st position (0-*0*001110). Here, the reference bit is shown in *italics*, while the identified 0/1 bit is shown in **bold**. Now that the reference bit has been detected as (0-100**1**110), the next 0 value appears at 0th position and the code-word is saved as (00-1, 0).With the reference to above-identified locations, next 0 is located in the 3rd position (0-100/110), following that, there are no 0s. Therefore, the code-word is finally determined to be (00-1, 0, 1 1).

Afterward, a 1-bit traversal is started, and the control bit is saved as 01. Similar to a technique used in the 0-bit traversal, it uses the initial bit as a reference bit to find presence of 1, which is identified at 0th position(0-*1*001110), and the code-word will be saved as (01-0). Following that, the procedure now restarts with recognized bit as the reference bit. The subsequent 1 rate seems at the 2nd location (0-100**1**110), and code-word is saved as (01- 0, 10). Next, 1 is identified at 0th position (0-100**1**/10), and other 1 seems at 0th location (0-1001**1**/0) with the reference to formerly recognized locations. As a result, final code-word attained using 1-bit traversal is

(01- 0, 10, 0, 0). When comparing the two code-words, the size of the code-word generated by ‘0’ and ‘1’ bits is 4 and 5 respectively. Thus, a 0-bit traversal-based code-word is selected as an ideal code-word (i.e., 00-1, 0, 11) and length of ideal code-word is updated for decompression.

In second level, the ideal code-word is considered input for position-enabled traversal to reduce the bits. The initial bit of the ideal code-word is 1, so the control bit is denoted as 10 for ‘0-bit traversal and finds the presence of 0s. Here 0s are present in only one position (i.e., 0th position (1-011)), so the code-word is (10-0). Likewise, for 1-bit traversal, the control bit is denoted as 11 and it uses the initial bit as a reference bit to find the presence of 1, which is identified at 1st position (1-011) and the next 1 at 0th position (1-01/). The code-word should be determined as (11-1, 0). Based on the number of bits, the optimal code-word is (10- 0).

During decoding procedure, control bit is initially examined to determine whether optimal code-word follows a 0-bit traversal or 1-bit traversal, as well as the value (0/1) of first bit in binary order. Every position in the code-word is filled with 0 when it is 0-bit traversal and 1 for the remaining positions. The code-word (10-0) will be decoded as follows; the control bits suggest that the sequence begins with 1, which is based on 0-bit traversal. The ideal code-word length is 4, so the sequence should be 1*** (4 bits). The first bit in the optimal code-word indicates the 0th position (10-**0**) and, with regards to first bit, 0th place will be = second bit, and also decoded order will be

10**. The rest of bits are filled with 1 and provide the ideal 4-bit code-word 1011.

In second-level decompression, control bits suggest that sequence begins with 0, and it is based on 0-bit traversal. The first bit is occupied with 0 and recreated code-word should be 0***** (8 bits). The first bit in code-word indicates the 1st position (00-1, 0, 11) and, with regards to first bit, 1st location will be third bit, and decoded series will be 0*0*****. Similar to this, the second bit in the code-word (00-1, 0, 11), denotes the 0th position and, in relation to the fourth bit, the reconstructed code-word should be 0*00****. Similarly, last bit in code-word signifies the 0th position (00-1, 0, 11) and, with regards to reference bit, 3rd position will be eighth bit, and decoded order will be 0*00***0. Finally, the rest of the bits are filled with 1 and provide the 8-bit binary sequence 01001110.

The binary rate is transformed into numeric rate of 78, and it corresponds to image's original pixel rate. This example demonstrates how the proposed algorithm improves compression performance while retaining effective reconstruction image quality, which will consume less energy due to the reduced number of bits for transmission in UWSN.

Algorithm 1: Proposed Two Layer Binary Traversal based Optimal Image Compression

```

1 Start
2 select input image A with  $a_{rc}$  pixels for
  compression
3 convert image into pixel lies between 0-255
4 find 8-bit binary equivalent for all pixels
5 //first-level code-word generation
6 //position enabled binary traversal
7 0-bit traversal  $Z_1$ 
8 1-bit traversal  $O_1$ 
9 update traversal count,  $Tr_c$ 
10 //ideal code-word selection
11 If length ( $Z_1$ ) < length( $O_1$ )
12 ideal code-word is  $Z_1$ 
13 else
14 ideal code-word is  $O_1$ 
15 end if
16 //second-level code-word generation
17 if  $O_{cw1} \geq O_{cw_{th}}$ 
18 //position enabled binary traversal
19 0-bit traversal  $Z_2$ 
20 1-bit traversal  $O_2$ 

```

```

21 update traversal count,  $Tr_c$ 
22 end if
23 //optimal code-word selection
24 If length ( $Z_2$ ) < length( $O_2$ )
25 optimal code-word is  $Z_2$ 
26 else
27 optimal code-word is  $O_2$ 
28 end if
29 run length encoding (bit: length)
30 End

```

Algorithm 2 : Compression algorithm in UWSN

```

1 Start
2 set UWSN sensor nodes
3 sensing underground colour images
4 convert image into 2D image A with  $a_{rc}$  pixels for
  compression
5 proposed two-layer binary traversal based
  optimal Image Compression
6 transfer compressed data to destination
7 reconstruction of image (i.e., decompression)
8 end

```

3 Results and Discussion

The results and discussion of devised image compression approach is specified in this section. Moreover, dataset description, sample images, performance analysis and comparative analysis are represented in this section.

3.1 Dataset

Underwater Image Enhancement Benchmark (UIEB) is considered to demonstrate the efficiency of the proposed compression algorithm (accessible at https://lichongyi.github.io/proj_benchmark.html). The dataset contains 890 raw underwater images and considers 50 test images for compression in UWSN. Some sample images from the dataset are depicted in Fig. 6.

3.2 Performance analysis

Here, the analysis is made for different sample images using various performance measures, namely MSE, SNR, SSIM, PSNR, and MAE and it is represented in the below Fig. 7 and Table 2.

3.2.1 Compression and Decompression time

Compression time is defined as time required compresses the original image, whereas decompression time is referred as time needed for decompression process.



Fig. 6 — Sample test images from UIEB.

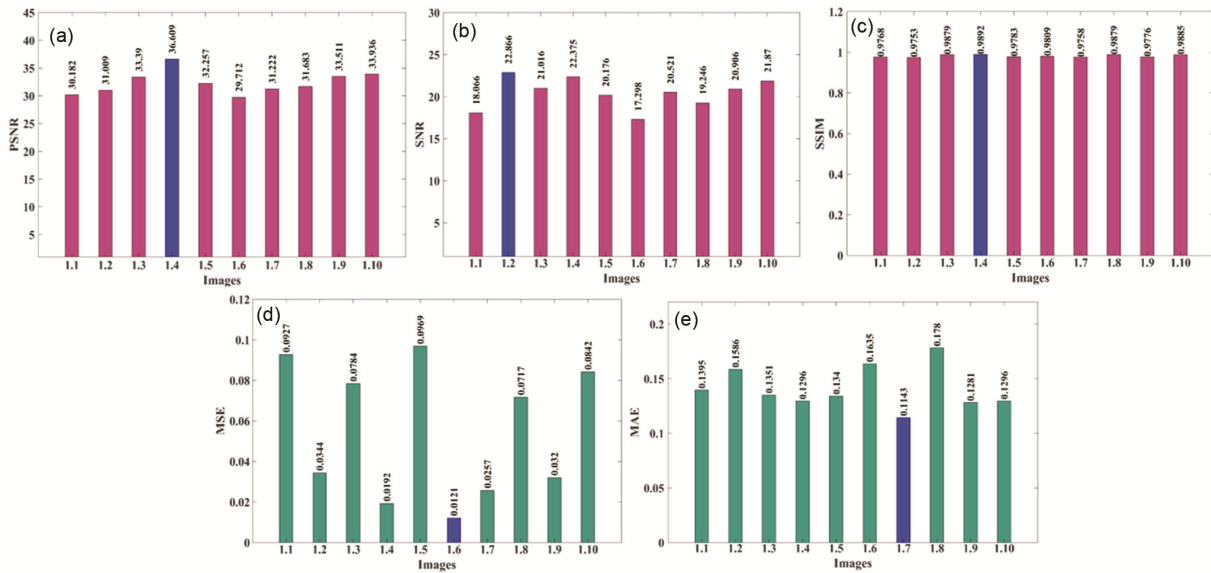


Fig. 7 — Performance analysis for sample images with various performance metrics (a) PSNR, (b) SNR, (c) SSIM, (d) MSE, and (e) MAE

Table 2 — Performance analysis

Images	PSNR	SNR	SSIM	MSE	MAE
<i>Image_1.1</i>	30.182	18.066	0.9768	0.0927	0.1395
<i>Image_1.2</i>	31.009	22.866	0.9753	0.0344	0.1586
<i>Image_1.3</i>	33.390	21.016	0.9879	0.0784	0.1351
<i>Image_1.4</i>	36.609	22.375	0.9892	0.0192	0.1296
<i>Image_1.5</i>	32.257	20.176	0.9783	0.0969	0.1340
<i>Image_1.6</i>	29.712	17.298	0.9809	0.0121	0.1635
<i>Image_1.7</i>	31.222	20.521	0.9758	0.0257	0.1143
<i>Image_1.8</i>	31.683	19.246	0.9879	0.0717	0.1780
<i>Image_1.9</i>	33.511	20.906	0.9776	0.0320	0.1281
<i>Image_1.10</i>	33.936	21.870	0.9885	0.0842	0.1296
<i>Mean</i>	32.351	20.434	0.982	0.0550	0.141

3.2.2. Space saving

It is computed from the original and compressed image size. This measure is referred as percentage of energy contributed through every block and it is computed by below expression,

$$SS = 100 \times \left(1 - \left[\frac{BC}{BU} \right] \right) \dots(4)$$

Here, *BC* refers to number of bits in compressed data and *BU* is amount of bits in uncompressed data.

3.2.3 Compression ratio

The compression ratio formula is typically expressed as the ratio of the size of the uncompressed data to the size of the compressed data. It can be calculated using the following formula:

$$CR(u, v) = \frac{size(M(u,v))}{size(M^*(u,v))} \dots (5)$$

where, $M(u, v)$ is original image and $M^*(u, v)$ denotes compressed image.

3.2.4 SSIM

It is used to calculate similarity among two images, which compares local patterns of pixel intensities, which have been normalized for contrast and luminance.

$$SSIM(u, v) = \frac{(2\chi_u\chi_v + H_1)(2\psi_{uv} + H_2)}{(\chi_u^2 + \chi_v^2 + H_1)(\psi_u^2 + \psi_v^2 + H_2)} \dots (6)$$

where, χ_u and χ_v is mean rate of luminance in original and decompressed image, ψ_u and ψ_v implies standard deviation of luminance, H_1 specifies contrast rate of original image and H_2 denotes contrast value of decompressed image.

3.2.5 SNR

The signal to noise ratio, or SNR, is statistic used for evaluating distortion. This is used to calculate how much the original image (u) has changed from the compressed and uncompressed version (v). Based on mean square error, SNR is calculated by,

$$SNR = 10 \log \left(\frac{\sum_{u=1}^{C_q-1} \sum_{v=1}^{C_w-1} M(u, v)^2}{\sum_{u=1}^{C_q-1} \sum_{v=1}^{C_w-1} |M(u, v) - M^*(u, v)|^2} \right) \dots (7)$$

3.2.6 PSNR

It is used to compute the effectiveness of compression, which is evaluated by,

$$PSNR(M, N) = 10 \log_{10} \left(\frac{F^2}{\frac{1}{C_q C_w} \sum_{u=1}^{C_q} \sum_{v=1}^{C_w} |M(u, v) - N(u, v)|^2} \right) \dots (8)$$

where, F refers maximal rate on one pixel, (C_q, C_w) is amount of pixels in q and w axis of image, M specifies original image and N defines reconstructed image.

3.2.7 MAE

MAE is evaluated by error between original and reconstructed images which is estimated by,

$$MAE = \max |M(u, v) - M^*(u, v)| \dots (9)$$

where, $M(u, v)$ is original image and $M^*(u, v)$ denotes compressed image.

3.2.8 MSE

MSE is calculated for finding actual difference among reconstructed and original images and it is non-negative integer. It is calculated by,

$$MSE = \frac{1}{H \times R} \sum_{k=1}^H \sum_{l=1}^R (g_{kl}^1 - g_{kl}^2)^2 \dots (10)$$

here, g_{kl}^1 implies pixel rate of original image and g_{kl}^2 denotes pixel value of reconstructed image.

The PSNR value is 30.182 for image 1.1, whereas PSNR rate is high as 36.609 for image 1.4 and the mean value for total 10 images is 32.351. Moreover, the SNR is varied from 17.298 to 22.866 for 10 images and its mean rate is 20.434. The SSIM value obtained by image 1.2 is 0.9753, and image 1.10 is 0.9885 and its mean is 0.982. The minimal MSE is 0.0121 for image 1.6 and minimal MAE is 0.1143 for image 1.6 and mean value of MSE and MAE is 0.0550 and 0.141.

3.3. Analysis for bandwidth

The bandwidth analysis for developed model with and without compression with regards to time is displayed in Fig. 8. During data transmission from sensor nodes to base station in UWSN, bandwidth is a crucial factor, which significantly affects the network's overall performance. It is ideal to choose a compression technique that uses less bandwidth since it improves the network's overall effectiveness. The maximum bandwidth used to transmit data before compression is 220.1142KB/. Moreover, the maximum bandwidth used to transmit data through designed compression scheme is 287.17696KB/s, which is much lesser than band width utilized for transmitting data without compression.

3.4. Comparative analysis

In this section, comparative analysis is performed for various existing methods based on performance measures, like PSNR, SNR, SSIM, MSE, MAE, compression ratio, compression, and decompression time and also space saving.

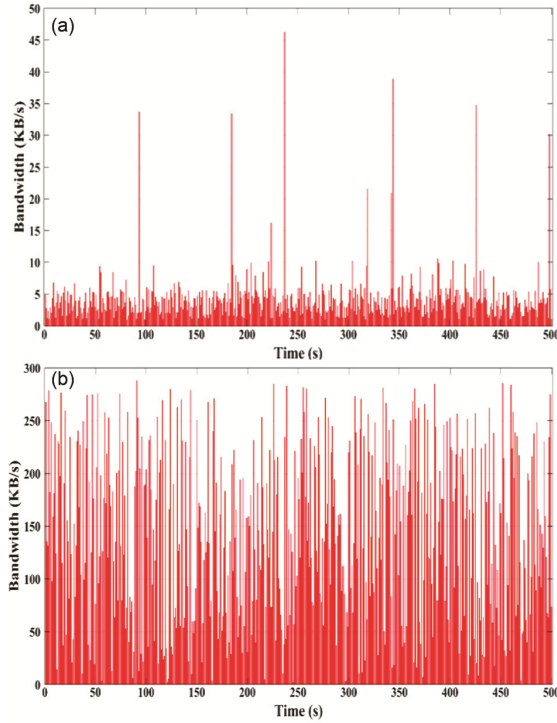


Fig. 8 — Bandwidth analysis for proposed approach (a) with compression, and (b) without compression

The comparative discussion for various existing methods with proposed approach based on performance metrics is deliberated in this section and it is shown in the below Table 3. The compression time for existing techniques and proposed model is 8.258s, 10.383s, 9.9613s, 20.7817s, and 5.426s, whereas decompression time is 9.984s, 10.8421s, 20.025s, 21.895s, and 5.064s. The proposed model has compression ratio of 2.0294, while space saving is 83.582%. The PSNR varies from 29.622 to 32.351 meanwhile, SNR changes from 18.236 to 20.434. The SSIM existing methods and proposed approach is 0.9642, 0.94756, 0.9025, 0.855, and 0.982. The MAE and MSE value of proposed image compression method is 0.0550 and 0.141.

By comparing the performance of the proposed technique with existing compression methods, such as Coefficient Permutation ABCS¹, Energy-based ABCS¹¹, MFHWT – ABCS¹⁷, Fuzzy-based ABCS⁶, shows on its suitability and effectiveness of the proposed method for underwater wireless sensor nodes in ecosystem monitoring applications.

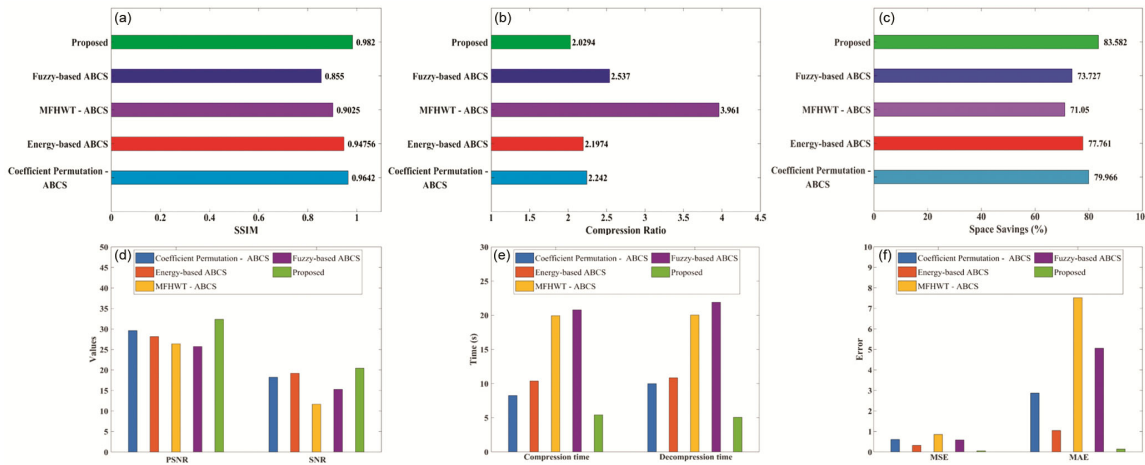


Fig. 9 — Comparative analysis for proposed method using performance metrics (a) SSIM, (b) Compression ratio, (c) Space saving, (d) PSNR and SNR, (e) Compression time and Decompression time, and (f) MSE and MAE

Table 3 — Comparison analysis

Metrics	Coefficient Permutation ABCS	Energy-based ABCS	MFHWT - ABCS	Fuzzy-based ABCS	Proposed
Compression time (s)	8.258	10.383	19.9613	20.7817	5.426
Compression ratio	2.242	2.1974	3.961	2.537	2.0294
Decompression time (s)	9.984	10.8421	20.025	21.895	5.064
Space Saving (%)	79.966	77.761	71.05	73.727	83.582
PSNR	29.622	28.1428	26.391	25.7302	32.351
SNR	18.236	19.195	11.661	15.279	20.434
SSIM	0.9642	0.94756	0.9025	0.855	0.982
MSE	0.6116	0.3231	0.8559	0.585	0.0550
MAE	2.872	1.0454	7.519	5.0564	0.141

4 Conclusion

In this article, optical threshold enabled image compression model is developed for UWSN. This approach mainly comprises of two layers, in first layer position-based binary traversal model was employed offers code-word. The threshold rate is employed for reducing bit as well as it affords optimum code-word. Besides, two-layer optimum code-words are encoded through run length encoding for improving compression and creates compressed data for transmission process. Moreover, optimal threshold driven image compression approach offers optimum bandwidth utilization. In addition, performance of compression is enhanced, when diminishing energy consumption in sensor nodes. The performance of proposed optimal threshold enabled image compression scheme is evaluated using various performance measures. The proposed technique achieved improved performance with compression time of 5.426s, decompression time of 5.064s, compression ratio of 2.0294, MAE of 0.141, MSE of 0.0550, PSNR of 32.351, SSIM of 0.982, and SNR of 20.434. Furthermore, the proposed approach will be further improved by including IoT for managing constrained resources.

References

- 1 Arjunan S & Pothula S, *Journal of King Saud University-Computer and Information Sciences*, 31 (2019) 304-317.
- 2 Uthayakumar J, Elhoseny M & Shankar K, *IEEE Transactions on Reliability*, 69 (2020) 1398-1423.
- 3 Majid M, Habib S, Javed A R, Rizwan M, Srivastava G, Gadekallu T.R. & Lin J C W, *Sensors*, 22 (2022) 2087.
- 4 Tavli B, Bicakci K, Zilan R & Barcelo-Ordinas, J.M., *Multimedia Tools and Applications*, 60 (2012) 689-726.
- 5 Charalampidis P, Fragkiadakis A G and Tragos E Z, *IEEE 81st Vehicular Technology Conference*, (2015) 1-5.
- 6 Nayak D, Ray K, Kar T & Mohanty S N, *Mathematics*, 11 (2023) 1660.
- 7 Monika R, Dhanalakshmi S, Kumar R & Narayanamoorthi R, *IEEE Sensors Journal*, 22 (2021) 776-784.
- 8 Felemban E, Shaikh F K, Qureshi U M, Sheikh A A & Qaisar S B, *International Journal of Distributed Sensor Networks*, 11 (2022) 896832.
- 9 Nguyen N T, Le T T, Nguyen H H & Voznak M, *Sensors*, 21 (2021) 627.
- 10 Han G, Jiang J, Shu L, Xu Y & Wang F, *Sensors*, 12 (2012) 2026-2061.
- 11 Monika R, Samiappan D & Kumar R, *The Visual Computer*, 37 (2021) 1499-1515.
- 12 Krishnaraj N, Elhoseny M, Thenmozhi M, Selim M M & Shankar K, *Journal of Real-Time Image Processing*, 17 (2020) 2097-2111.
- 13 Durrani M Y, Tariq R, Aadil F, Maqsood M, Nam Y & Muhammad K, *Sensors*, 19 (2019) 1145.
- 14 Hong Z, Pan X, Chen P, Su X, Wang N & Lu W, *Sensors*, 18 (2018) 2306.
- 15 Yu W, Chen Y, Wan L, Zhang X, Zhu P & Xu X, *IEEE Access*, (2020) 89171-89184.
- 16 Hou R, He L, Hu S & Luo J, *IEEE Access*, 6 (2018) 39685-39691.
- 17 Monika R, Hemalatha R & Radha S, *Multimedia Tools and Applications*, 77 (2018) 30187-30203.
- 18 Ahmed A J, Hamdi M M, Mustafa A S & Rashid S A, *IEEE International Congress on Human-Computer Interaction*, (2022) 1-4.
- 19 Nair R S & Domic S, *International Journal of Information Technology*, (2022) 1-12.
- 20 Yadav S & Kumar V, *SVD, Progress In Electromagnetics Research Letters*, 109 (2023) 15-22.
- 21 Anjum K, Li Z & Pompili D, *IEEE Sixth Underwater Communications and Networking Conference*, (2022) 1-5.
- 22 Nilsaz Dezfouli N & Barati H, *IET Communications*, 13 (2019) 578-584.
- 23 Hatamian M, Bardmily M A, Asadboland M, Hatamian M & Barati H, *Radioengineering*, 25 (2016) 114-123.
- 24 NilsazDezfouli N & Barati H, *Wireless Networks*, 26 (2020) 1839-1855.
- 25 Hatamian M, Barati H, Movaghar A & Naghizadeh A, *Telecommunication Systems*, 62 (2016) 657-674.
- 26 Ghorbani Dehkordi E & Barati H, *International Journal of Electronics*, 1-13.
- 27 Papi F & Barati H, *International Journal of Communication Systems*, 35 (2022) 5120.
- 28 Akbari M R, Barati H & Barati A, *Wireless Networks*, 28 (2022) 521-538.
- 29 Kiamansouri E, Barati H & Barati A, *Peer-to-Peer Networking and Applications*, 15 (2022) 2142-2159.
- 30 Akbari M R, Barati H & Barati A, *Computing*, 104 (2022) 1307-1335.
- 31 Manikandan T T, Sukumaran R, Raj M C & Saravanan M, *IEEE 4th International Conference on Electronics, Communication and Aerospace Technology (ICECA)*, (2020) 695-701.